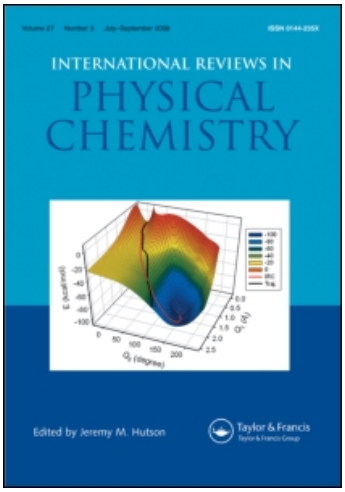

International Reviews in Physical Chemistry
Publication details, including instructions for authors and subscription information:
http://www.informaworld.com/smpp/title~content=t713724383

Reactions of NO with nitrogen hydrides x

A. M. Mebel; M. C. Lin

Online publication date: 26 November 2010

To cite this Article Mebel, A. M. and Lin, M. C.(1997) 'Reactions of NO with nitrogen hydrides x', International Reviews in Physical Chemistry, 16: 2, 249 — 266
To link to this Article: DOI: 10.1080/014423597230299
URL: http://dx.doi.org/10.1080/014423597230299

INTERNATIONAL REVIEWS IN PHYSICAL CHEMISTRY, 1997, VOL. 16, NO. 2, 249–266

Reactions of NO_x with nitrogen hydrides

by A. M. MEBEL

Institute of Atomic and Molecular Sciences, Academia Sinica, PO Box 23-166, Taipei 10764, Taiwan

and M. C. LIN†

Department of Chemistry, Emory University, Atlanta, GA 30322, USA

In this review, we consider the reactions of NO_x (x = 1,2) with the nitrogen hydrides NH, NH_2 and NH_3. The reactions are relevant to the post-combustion, non-catalytic reduction of NO_x with NH_3 in the thermal de-NO_x process and with HNCO in the rapid reduction of NO_x as well as to the thermal decomposition of some high-energy materials, including ammonium dinitramide. The practical importance has motivated considerable theoretical interest in these reactions. We review numerous *ab-initio* molecular orbital studies of potential energy surfaces for $NO_x + NH_y$ and theoretical calculations of their kinetic parameters, such as thermal rate constants and branching ratios of various products. The most advanced theoretical calculations are carried out using the Gaussian-2 family of methods which provides the chemical accuracy (within 2 kcal mol^{-1}) for the energetics and molecular parameters of the reactants, products, intermediates and transition states. We present a detailed comparison of the theoretical results with available experimental data. We show that the reactions of NO_x with NH and NH_2 are very fast because they occur without a barrier and lead to the formation of multiple products which include radicals and stable molecules. The reactions of NO_x with NH_3, taking place by the H abstraction to form NH_2 and HNO_x, are slow but still relevant to the NH_3 de-NO_x system, because of their fast reverse processes which have not yet been measured experimentally.

1. Introduction

Recent heightened environmental concerns have motivated much theoretical interest in the chemistry of NO_x, particularly in their post-combustion, non-catalytic reduction with NH_3 in the thermal de-NO_x process [1] and with HNCO in the rapid reduction of NO_x [2]. These well known non-catalytic reduction processes utilize the highly efficient reducing capabilities of the NH_x (x = 1, 2) radicals which are generated in the high-temperature (1200–1400 K) reduction processes by chain reactions of NH_3 and HNCO with H and OH. The $NH_x + NO_x$ reactions are also relevant to the mechanism of the thermal decomposition of ammonium dinitramide (ADN) ($NH_4N(NO_2)_2$) [3] which is a Cl-free high-energy material and a potential replacement for ammonium perchlorate, possibly with reduced plume signature and stratospheric ozone destruction [4].

The reactions of NO_x with NH and NH_2 take place without a barrier with very large rate constants [5]. As will be discussed in subsequent sections, these reactions often lead to the formation of multiple products which include radicals and stable molecules. Multiple-product formation results from the facile H migration from the N site of NH_x to the N and/or O sites of NO_x in the chemically activated association

† Corresponding author; e-mail: chemmcl@emory.edu.

0144–235X/97 $12·00

intermediates. For example, the internally excited intermediate $H_2NNO_2^{\dagger}$ formed in the $NH_2 + NO_2$ reaction, can isomerize to give various isomers of $HNN(O)OH^{\dagger}$ which can, in turn, undergo exothermic fragmentation reactions, producing $N_2O + H_2O$.

Numerous experimental and theoretical studies have been conducted on the reaction of NO_x with nitrogen hydrides (NH_y, y = 1–3) as will be cited in our discussion of the individual processes. Despite the enormous progress made in theory, quantitative prediction of their absolute rate constants and product branching probabilities over a wide range of experimental conditions, particularly for the barrierless association–decomposition processes, such as $NH_x + NO_x$ (x = 1, 2), is still difficult, as can be seen from the discussion.

This review begins with the discussion of the Gaussian-2 (G2) method put forward by Pople and co-workers [6]. This method, particularly the modified version by Mebel *et al.* [7], has been employed extensively by us for *ab-initio* calculations of a variety of chemical reaction systems involving species of up to six or seven heavy atoms.

Following the brief review of the computation techniques, we shall discuss the results of the $NH_x + NO_x$ (x = 1, 2) reactions obtained in recent high-level *ab-initio* molecular orbital (MO) calculations. In view of the fact that the reactions of NO_x and NH_3, particularly their reverse processes $NH_2 + HNO$ and $NH_2 + HONO$, are relevant to the NH_3 de-NO_x system, we have performed various levels of the Gaussian calculations for the two metathetical reactions. These results will also be reviewed.

2. Accurate *ab-initio* molecular orbital calculations of potential energy surfaces: Gaussian-2 theoretical models

When *ab-initio* MO calculations are used to study potential energy surfaces (PESs) of chemical reactions, such as $NH_x + NO_x$ considered in the present review, the reliability of the results is critical. On account of the great progress made in the field of computational chemistry in recent years, it is now possible to perform calculations of PESs for the reactions between small molecules and radicals to chemical accuracy. The G2 series of methods were developed with the goal of achieving the prediction of molecular energies to within 2 kcal mol^{-1}. The original G2 methodology elaborated by Pople and co-workers [6] uses a series of QCISD(T) [8], MP4 and MP2 [9] calculations with various basis sets to approximate a QCISD(T)/6-311 + G(3df, 2p) calculation with an additional empirical 'higher-level correction' based on the number of paired and unpaired electrons. The geometry in G2 is optimized at the MP2/6-31G(d) level and vibrational frequencies are calculated by HF/6-31G(d). For this method, the average absolute deviation of calculated atomization energies from experiment for 32 first-row compounds is 0·92 kcal mol^{-1}.

Various modifications of G2, aimed to improve its performance for transition states and for radical species, were proposed later. Durant and Rohlfing [10] suggested optimization of the geometry and calculation of vibrational frequencies using the QCISD/6-311G(d, p) approach. This method, called G2Q, refined performance in predicting transition state energies. However, the calculations of geometries and, especially, frequencies at the QCISD level are extremely expensive and the G2Q scheme, although reliable, is not practical for species containing more than three non-hydrogen or heavy atoms.

Recent developments in density functional theory enabled one to modify and improve further the performance of G2. We proposed [7] optimization of geometries and calculation vibrational frequencies using the hybrid density functional B3LYP/6-

311G(d, p) approach, that is Becke's [11] three-parameter non-local exchange (B3LYP) functional in conjunction with the nonlocal correlation functional of Lee *et al.* [12]. In most cases, the B3LYP approach is as accurate but much more effective than QCISD for the calculations of geometries and frequencies. The use of B3LYP instead MP2 for the frequency calculations is critical for radical species where UMP2 can lead to unexpectedly large errors caused by spin contamination. From a comparison of the transition state energies for various radical reactions calculated by QCISD(T), the restricted open-shell-coupled-cluster (RCCSD(T)) and the multi-reference MRSD-CI methods, we found that the RCCSD(T) results agree better with the most reliable MRSD-CI ones than those from QCISD(T) calculations. Therefore, we suggested to replace the QCISD(T) calculation in the G2 scheme by RCCSD(T). We called the series of the modified G2 methods G2M [7]. Thus, G2M uses a series of RCCSD(T), MP4 and MP2 calculations to approximate a RCCSD(T)/6-311+G(3df, 2p) energy, where geometries and vibrational frequencies are calculated at the B3LYP/6-311G(d, p) level of theory. The most accurate model, called G2M(RCC), gives the average absolute deviation of calculated atomization energies of 0·88 kcal mol^{-1} from experiment for 32 first-row compounds. The other methods, G2M(RCC, MP2) and G2M(rcc, MP2), exhibit average absolute deviations of 1·15 and 1·28 kcal mol^{-1} respectively and can be used for the calculations of molecules and radicals of larger sizes containing up to six or seven heavy atoms. The preference of G2M over the original G2 method is expected to be particularly significant for open-shell systems with large spin contamination. The G2M approach has been successfully tested for various radical reactions relevant to combustion [13–16].

3. $NH + NO_x$ reactions

3.1. $NH + NO$

Considering the $X\,^3\Sigma^-$ ground state of NH, there are two exothermic product channels for the NH + NO reaction:

$$NH(X\,^3\Sigma^-) + NO \rightarrow N_2 + OH, \quad \Delta H = -97{\cdot}6 \text{ kcal mol}^{-1}, \tag{1a}$$

$$\rightarrow N_2O + H, \quad \Delta H = -34{\cdot}7 \text{ kcal mol}^{-1}. \tag{1b}$$

The reaction rate coefficient has been studied near room temperature [17–22], in shock-heated gases [23, 24] and in flames [25, 26]. Low-temperature rates, reported to be temperature-independent for the temperature range of 269–377 K [20], vary within the values $k(298\text{ K}) = (3{\cdot}8\text{–}5{\cdot}8) \times 10^{-11}$ cm^3 molecule^{-1} s^{-1}. High-temperature rate coefficients of $k(2200\text{–}3350\text{ K}) = 2{\cdot}8 \times 10^{-10} \exp(-6400/T)$ cm^3 molecule^{-1} s^{-1} [22] and $k(3500\text{ K}) = (1{\cdot}3 \pm 0{\cdot}1) \times 10^{-10}$ cm^3 molecule^{-1} s^{-1} [24] have been reported. Some direct studies have examined the product branching ratio for reaction (1). Harrison *et al.* [20] looked for the OH product with laser-induced fluorescence (LIF) but did not detect any. Despite this, they concluded that $N_2 + OH$ were probably the major products of the reaction [20]. Using the discharge flow technique, Durant and co-workers [27–29] measured the product branching ratio at room temperature for the production of $N_2O + H(D)$ to be $0{\cdot}84 \pm 0{\cdot}4$ for $NH(X\,^3\Sigma^-) + NO$ and $0{\cdot}87 \pm 0{\cdot}17$ for $ND(X\,^3\Sigma^-) + NO$. Matsui and co-workers [21, 22] also attempted to measure the branching ratio of the reaction. In their more direct measurement, using HNCO as the NH precursor [22], they concluded that the branching ratio for channel (1*a*) was 0·30 and for channel (1*b*) 0·65 with the balance for unspecified products. This value appears

to be consistent with the result of Mertens *et al.* [23] for equation (1*a*), 0·27 ± 0·10 at 2350 K ⩽ T ⩽ 3040 K, which is also in good agreement with the result of Yokoyama *et al.* [24], 0·32 ± 0·07 at 3500 K. Quandt and Hershberger [30] measured N_2O formation by diode laser absorption spectrometry at 298 K. Their result gave 0·77 ± 0·08 for the branching ratio of its production, which is in reasonable agreement with the findings of Matsui and co-workers [22] and Durant [27] mentioned above.

Unlike many other reactions of NH where the $^1\Delta$ state is more reactive, the NH + NO reaction has comparable rates for the ground X $^3\Sigma^-$ state and the low-lying $^1\Delta$ state of NH. Matsui and co-workers [22] found that the NH ($^1\Delta$) + NO reaction led predominantly to electronic quenching:

$$NH(^1\Delta) + NO \rightarrow NH(^3\Sigma^-) + NO,$$

with a branching ratio of 0·57, while those for the formation of N_2O and N_2 were determined to be 0·20 and 0·14, respectively.

The product energy distribution for channel (1*a*) has been studied by Patel-Mistra and Dagdigian [31] in a crossed-beam experiment. The OH v = 1 to 0 vibrational population ratio was found to be 0·30 ± 0·06 and the average rotation energy about 6 kcal mol^{-1}. These workers noted that this is a small amount of internal excitation given that the reaction is exothermic by 97·6 kcal mol^{-1}. The study of Böhmer *et al.* [32] on the reaction of N_2O with hot H atoms formed by photolysis of an N_2O–HI complex, is in general agreement with the work of Patel-Mistra and Dagdigian regarding the OH internal energy distribution, but the OH Doppler shift profiles in these experiments require a large amount of internal vibrational excitation of N_2 (71·5 kcal mol^{-1} for OH v = 0). This result is explained by a model in which the HNNO complex has an elongated NN bond and the 1,3-H shift is assumed to occur rapidly with respect to motion of the heavy atoms, leaving the N_2 product vibrationally excited.

There have been a number of theoretical studies of the potential energy surface for NH + NO. Melius and Binkley [33] and Miller and Melius [34] used the bond-additivity-corrected (BAC) MP4 perturbation method to calculate reactants, products, intermediates and transition states. Fueno *et al.* [35] used MRD-CI//HF/4-31G(d, p) to calculate energies of stationary points on the HNNO $^2A'$ surface as well as the energies of the *cis* and *trans* isomers of HNNO $^2A''$, which were predicted to lie higher than the $^2A'$ states of the two isomers. Harrison and Maclagan [36] reported the HF, MP2 and MP4 calculations for the reaction. The most accurate calculations to date of the NH + NO PESs can be attributed to Walch [37] and Durant [27]. The profile of the PESs for NH + NO is shown in figure 1(*a*).

For the calculations, Walch used the CASSCF/internally contracted configuration interaction (ICCI) approach with Dunning's VDZ and VTZ basis sets. He carefully considered the first reaction step, the association of NH and NO to form HNNO. Combining the $^3\Sigma^-$ ground state of NH with the $^2\Pi$ ground state of NO and keeping a plane of symmetry leads to $^{2,4}A'$ and $^{2,4}A''$ surfaces. For the $^2A''$ surface, the singly occupied NO 2π orbital is in plane of the supermolecule and the addition of NH to NO occurs without barrier. However, the $^2A''$ surface is not correlated either to N_2 + OH or to H + N_2O products. Also, according to the calculations, the $^2A''$ isomers of HNNO lie 25–30 kcal mol^{-1} higher in energy than the $^2A'$ isomers. For the $^2A'$ surface, the singly occupied NO 2π orbital is perpendicular to the plane of the supermolecule, the NH is adding to an NO π bond, and a barrier for addition exists on this surface. On the other hand, the $^2A'$ surface is correlated with the N_2O + H and N_2 + OH

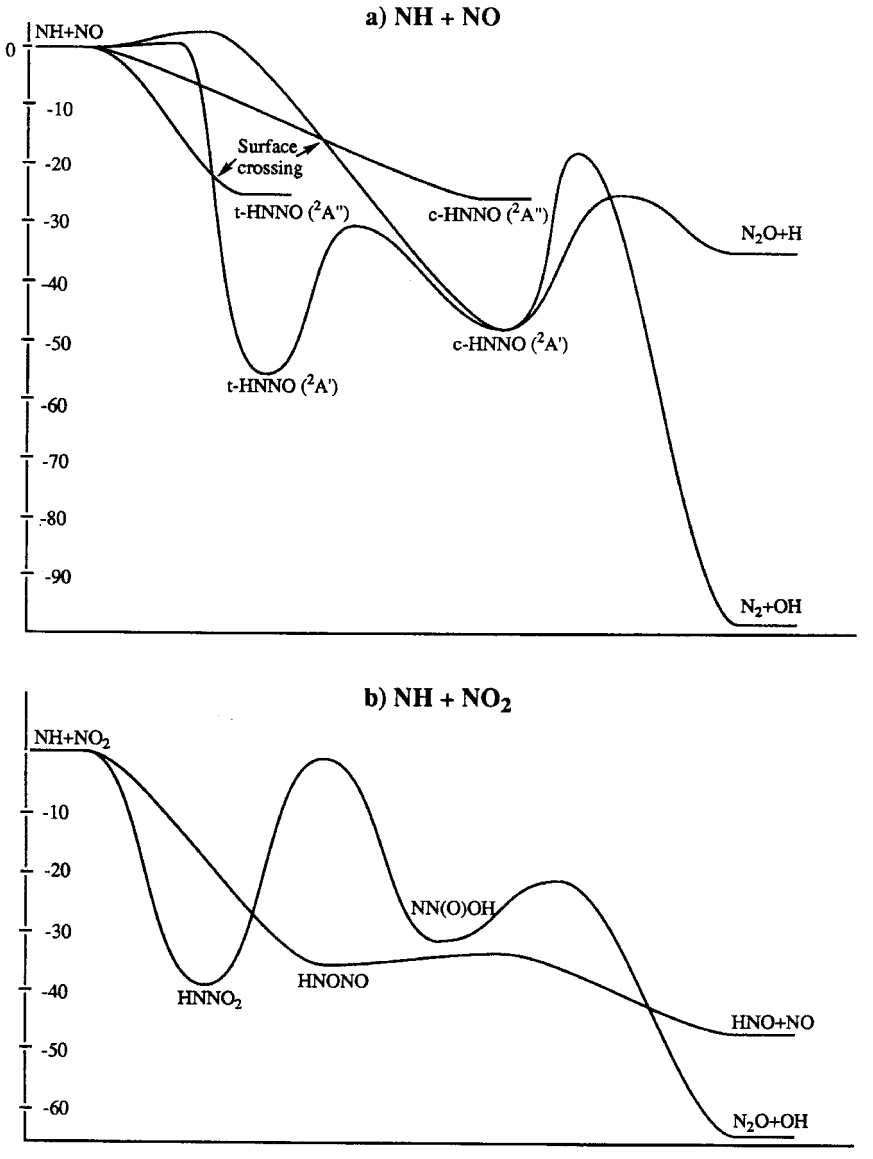

Figure 1. Calculated profiles of PESs for the reactions (*a*) NH + NO and (*b*) $NH + NO_2$. A more detailed PES of (*b*) can be found in [39] and [40].

products. There exists an entrance channel surface crossing between the $^2A''$ and $^2A'$ surfaces, which means that the HNNO ($^2A'$) association product is formed without barrier, by hopping between $^2A''$ and $^2A'$.

Both *trans*- and *cis*-HNNO ($^2A'$) can be formed during the association step. According to the CASSCF/ICCI results, they lie 51·2 and 46·2 kcal mol^{-1} respectively below the reactants. The more accurate G2Q calculations of Durant [27] give for *trans*- and *cis*-HNNO ($^2A'$) energies of −56·0 and −48·9 kcal mol^{-1} respectively. The *trans–cis* isomerization requires a significant barrier, 25·2 kcal mol^{-1} relative to *trans*-

HNNO at the G2Q level, but the transition state is still 30·8 kcal mol^{-1} lower than NH ($^3\Sigma^-$)+NO. *cis*-HNNO can either eliminate the H atom or form NNOH by the 1,3-H shift. The latter isomer is not stable and immediately dissociates to N_2+OH. The product branching ratio, N_2O+H as against N_2+OH, is controlled by the energies and molecular parameters of the transition states for H splitting and 1,3-H shift in HNNO. At the CASSCF/ICCI level, H–N_2O and N_2–OH transition states lie 21·4 and 15·4 kcal mol^{-1} below the reactants. The corresponding values at the G2Q and BAC-MP4 levels are 25·3 and 17·9 kcal mol^{-1} and 28·2 and 22·4 kcal mol^{-1}, respectively. Thus various theoretical methods predict the barrier for the H splitting to be lower than the barrier for the 1,3-H shift by 6–7 kcal mol^{-1}. On the basis of his G2Q calculations, Durant and co-workers [27–29] concluded that the reaction would predominantly form N_2O+H products. In the transition state for the 1,3-H shift, the NN bond is elongated by 0·11 Å compared with that in N_2, and Walch [37] as well as Böhmer *et al.* [32] attributed the production of vibrationally excited N_2 to this elongation. Miller and Melius [34] have performed branching ratio calculations using BAC-MP4 energies and predicted a branching fraction of 0·81 at 300 K for the N_2O+H channel, which is in good agreement with the experimental result of 0·84 obtained by Durant and co-workers [27–29]. The calculated value decreases slowly with temperature to 0·70 at 3500 K which also agrees quantitatively with the reported results of Mertens *et al.* [23] as well as those of Yokoyama *et al.* [24].

In general, the G2Q energetics obtained by Durant and co-workers agree well with the CASSCF/ICCI results of Walch, especially if one lowers Walch's surface by 3·3 kcal mol^{-1}, to match the CASSCF/ICCI exothermicity for the N_2O+H channel with the experimental value. The BAC-MP4 energies agree with those of G2Q with an accuracy of 3–5 kcal mol^{-1}.

Recently, Schatz and co-workers [38] studied the dynamics of the NH+NO reaction based primarily on Walch's [37] PES data. The result of this quasiclassical trajectory study predicted that about 13% of the reaction produced N_2+OH (or 87% N_2O+H) at 300 K. This is in good agreement with the Miller–Melius [34] statistical calculation result and the experimental value of Durant and co-workers.

Since the critical transition states for both N_2O+H and N_2+OH product channels lie much lower than the reactants, the total reaction rate constant for NH+NO is controlled by the initial association step. The association occurs without a barrier. Therefore, for accurate theoretical calculations of the total rate constant, a variational Rice–Ramsperger–Kassel–Markus (RRKM) approach is required, for which the study of the $^2A''$ and $^2A'$ attractive potentials would be necessary.

For the reaction of the excited state NH ($^1\Delta$) with NO, Fueno *et al.* [35] speculated that NH ($^1\Delta$) correlates with the $^2A'$ surface. However, according to Walch's [37] consideration, this model is substantially oversimplified. The addition of NH ($^1\Delta$) to NO involves a geometry in which the N atom of NH approaches near the midpoint of the NO bond with the NH bond perpendicular to the N-NO plane. Combining the $^3\Sigma^-$ and $^1\Delta$ states of NH with the $^2\Pi$ of NO leads to six PESs. The lowest two of them are the $^2A'$ and $^2A''$ surfaces which correlate with $^3\Sigma^-$. Of the remaining four surfaces, three are repulsive and one is attractive. The electronic configuration of the attractive state is analogous to the configuration involved in the insertion of O(^{1}D) into H_2. This configuration can correlate with N_2O+H. Fueno *et al.* also considered that the NH($^1\Delta$)+NO reaction may lead to the N_2H+O (^{3}P) and NH ($^3\Sigma^-$)+NO products. More careful study of the excited-state PES is required in order to predict the NH ($^1\Delta$)+NO rate constant and the product branching ratio.

3.2. $NH + NO_2$

There are three possible exothermic spin-allowed product channels for the reaction of NH ($^3\Sigma^-$) + NO_2:

$$NH + NO_2 \rightarrow N_2 + HO_2, \quad \Delta H = -92{\cdot}5 \text{ kcal mol}^{-1}, \tag{2a}$$

$$\rightarrow N_2O + OH, \quad \Delta H = -64{\cdot}1 \text{ kcal mol}^{-1}, \tag{2b}$$

$$\rightarrow NO + HNO, \quad \Delta H = -47{\cdot}8 \text{ kcal mol}^{-1}. \tag{2c}$$

Experimentally, this reaction was studied by Harrison *et al.* by LIF [20]. They obtained the rate constant at 300 K to be $(1{\cdot}61 \pm 0{\cdot}14) \times 10^{-11}$ cm^3 molecule^{-1} s^{-1} and found a small negative temperature dependence of the rate constant between 260 and 380 K. The product branching ratios of the reaction have been measured by Quandt and Hershberger [30] to be $0{\cdot}41 \pm 0{\cdot}15$ for channel (2*b*) and $0{\cdot}59 \pm 0{\cdot}15$ for channel (2*c*) at 298 K.

Harrison and Maclagan [36] reported *ab-initio* calculations of the $NH + NO_2$ reaction at the MP4(SDQ)//HF/6-311G(d p) level. This study could not explain the observed negative temperature dependence of the rate constant; the calculated transition state for $HNNO_2$ dissociation into N_2O and OH lies about 14 kcal mol^{-1} higher than the reactants.

More detailed and quantitative study of the $NH + NO_2$ potential energy surface was carried out by us at the QCISD(T)/6-311G(d, p) and G2 levels [39]. The profile of the potential energy surface is shown in figure 1 (*b*). We found that the reaction can occur by two channels. The first proceeds at the initial step by the HN–NO_2 association and leads to the $HNNO_2$ species. $HNNO_2$ undergoes a 1,3-H shift to form NN(O)OH. The latter eliminates OH, giving rise to the $N_2O + OH$ products. The association occurs without barrier, but the hydrogen shift step requires a high activation energy, about 37 kcal mol^{-1} at the QCISD(T)/6-311G(d, p) level. This value is higher than the barrier for the 1,3-H shift in *cis*-HNNO, 31 kcal mol^{-1} at the G2Q level [27]. The strength of the NN bond in HNNO, 56 kcal mol^{-1} at the G2Q level, is significantly higher than that in $HNNO_2$, 38 kcal mol^{-1} in a similar G2M approximation. The transition state for the 1,3-H shift in $HNNO_2$ lies above the reactants in the QCISD(T) approximation. However, G2 calculations lower the barrier and give for this transition state an energy 0·2 kcal mol^{-1} below the reactants. The barrier for the third step, OH elimination from NN(O)OH, is about 10 kcal mol^{-1}, with the transition state lying substantially lower than the reactants. Therefore, the energy of the transition state for the hydrogen shift is critical. According to the G2 results, the $NH + NO_2 \rightarrow HNNO_2 \rightarrow NN(O)OH \rightarrow N_2O + OH$ channel can exhibit a negative temperature dependence in the rate constant. In contrast with HNNO, $HNNO_2$ cannot dissociate exothermically to produce the H atom.

In comparison with the NH + NO reaction, an additional channel exists for $NH + NO_2$. The initial association can take place at the O end of NO_2 to form HNONO. According to our CASSCF calculations, the $HN + ONO \rightarrow HNONO$ reaction does not have a barrier. The HNONO intermediate, $-35{\cdot}5$ kcal mol^{-1} relative to $NH + NO_2$ at the G2M level, thermodynamically is almost as stable as $HNNO_2$. On the other hand, HNONO is unstable kinetically and exothermically it dissociates to HNO + NO, overcoming a low barrier of 1·0 kcal mol^{-1}. The $NH + NO_2 \rightarrow HNONO \rightarrow HNO + NO$ channel would also exhibit a negative temperature dependence in its rate constant. The other mechanism leading to HNO + NO, involving O migration in $HNNO_2$, is improbable owing to the high barrier for O shift.

As in NH + NO, a variational approach is required in order to describe the rate constants of the initial association steps in the $NH + NO_2$ reaction, leading to $HNNO_2$ and HNONO. The total rate constant should be calculated in terms of the variational RRKM theory. The prediction of the product branching ratio for $NH + NO_2$, that is HNO + NO as against $N_2O + OH$, is more complicated than for NH + NO because the product channels does not share the same association step and both association steps are barrierless. Accordingly, separate variational RRKM calculations are required for the two channels $NH + NO_2 \rightarrow HNNO_2 \rightarrow N_2O + OH$ and $NH + NO_2 \rightarrow HNONO \rightarrow HNO + NO$. These calculations require realistic interaction potentials for all barrierless transition states.

While the $N_2 + HO_2$ product channel is the most exothermic for $NH + NO_2$, these products cannot be formed directly in this reaction. $N_2 + HO_2$ can be produced in a secondary reaction between N_2O and OH. The reaction can take place by direct abstraction of the oxygen atom from N_2O. The barrier is high, 40·5 kcal mol^{-1} at the G2M level [40], and the $N_2O + OH \rightarrow N_2 + HO_2$ reaction is slow. The calculated rate constant in the temperature range 1000–5000 K is $2{\cdot}15 \times 10^{-26}\ T^{4{\cdot}72} \exp(-18\,400/T)$ cm^3 $molecule^{-1}$ s^{-1} [40].

4. $NH_2 + NO_x$ reactions

4.1. $NH_2 + NO$

Because of its great importance to combustion and particularly to the thermal de-NO_x process the reaction of NH_2 with NO has been the subject of numerous experimental studies and theoretical calculations. The major channels proposed by Silver and Kolb [41, 42] for the $NH_2 + NO$ reaction are the following:

$$NH_2 + NO \rightarrow N_2H + OH, \qquad \Delta H = 1 \text{ kcal mol}^{-1}, \tag{3a}$$

$$\rightarrow N_2 + H_2), \qquad \Delta H = -124{\cdot}9 \text{ kcal mol}^{-1}, \tag{3b}$$

$$\rightarrow N_2 + H + OH, \qquad \Delta H = -5{\cdot}7 \text{ kcal mol}^{-1}, \tag{3c}$$

$$\rightarrow H_2 + N_2O, \qquad \Delta H = -47{\cdot}5 \text{ kcal mol}^{-1}, \tag{3d}$$

Casewit and Goddard [43] used the generalized valence bond configuration interaction method with a polarized double-zeta basis set to study nine isomers of formula N_2H_2O, geometries of those were optimized at the RHF/4-31G level. Melius and Binkley [33] carried out an extensive calculation of this system using the BAC-MP4 approach. Abou-Rachid *et al.* [44] carried out CIPSI calculations for the reaction intermediates and transition states using RHF/6-31G optimized geometries. They concluded that the formation of molecular nitrogen is highly probable but the reaction pathway leading to $N_2H + OH$ cannot be thermodynamically excluded. Abou-Rachid *et al.* used their PES and molecular parameters to calculate the reaction rate constant by means of the RRKM and transition state theory (TST) methods. The computed rate coefficient $k_3 = 1{\cdot}64 \times 10^{-11}$ cm^3 $molecule^{-1}$ s^{-1} at 298 K appeared to be comparable with that determined experimentally and to exhibit a negative temperature dependence in the range 200–700 K. However, the theoretical rate constant deviates from experimental observations above 700 K. Harrison *et al.* [45] studied the $NH_2 + NO$ reaction at the MP4 (SDQ) level with HF/6-31G* geometry optimization. They found that the pathway leading to the production of N_2 and H_2O via intramolecular rearrangement of N_2H_2O species can occur with a small or no activation barrier and the channel to N_2H will be at most a secondary pathway, with the intermediate N_2H molecule dissociating rapidly to $N_2 + H$.

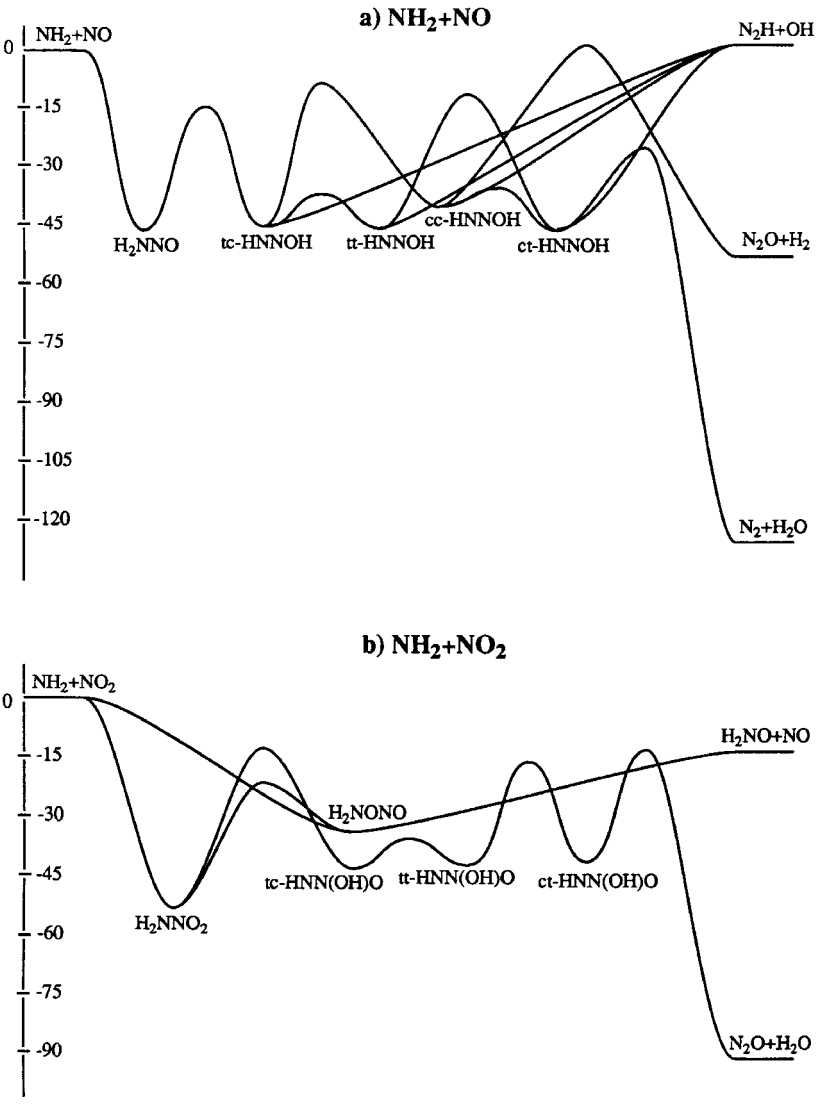

Figure 2. Calculated profiles of PESs for the reactions (*a*) NH_2+NO and (*b*) NH_2+NO_2. A more detailed PES of (*b*) can be found in [60].

Detailed and high level calculations of the PES for reaction (3) were carried out by Walch [46] as well as by Duan and Page [47]. The PES is summarized in figure 2(*a*). Walch used the ICCI method with the pVTZ basis set for the energy calculations, while geometries of the intermediates and transition states were optimized at the CASSCF/pVDZ level. Duan and Page performed MRCI/pVTZ/CASSCF/pVDZ calculations with a larger active space for CASSCF included 12 electrons distributed among 11 orbitals. According to the results of these calculations, the first step of the reactions is the formation of the vibrationally excited H_2NNO intermediate. This process occurs without barrier and H_2NNO lies 44 kcal mol^{-1} below the reactants. On the next step, a 1,3-H migration takes place with an energy barrier of 30–35 kcal mol^{-1} to give a *trans*, *cis*-HNNOH isomer (*trans* about the NN bond and *cis* about the NO bond). Another possibility is 1,1-H_2 elimination from H_2NNO to form H_2+N_2O.

However, Melius and Binkley [33] found that the barrier for the H_2 elimination is very high, about 80 kcal mol^{-1}. The *trans*, *cis*-HNNOH may isomerize along either the NN bond to form *cis*, *cis*-HNNOH (the barrier is 42·0 kcal mol^{-1}) or the NO bond to form *trans*,*trans*-HNNOH (the barrier is 8·8 kcal mol^{-1}). The *cis*,*cis*-HNNOH can undergo 1,3-H_2 elimination to form $N_2O + H_2$; however, this process has a high barrier of 49·8 kcal mol^{-1}. Both *cis*, *cis*- and *trans*, *trans*-HNNOH may also isomerize along either the NO bond or the NN bond to form *cis*, *trans*-HNNOH with barriers of 2·5 and 37–39 kcal mol^{-1} respectively. The *cis*, *trans*-HNNOH may further decompose exothermically with an energy barrier of 24–27·5 kcal mol^{-1} to form H_2O and N_2. Each HNNOH isomer may also decompose to produce OH and N_2H with exothermicity of about 45 kcal mol^{-1} and without any reverse barrier. For the most exothermic reaction channel, $NH_2 + NO \rightarrow H_2NNO \rightarrow$ *trans*, *cis*-HNNOH $\rightarrow$ $N_2 + H_2O$, the highest barrier is calculated for the *trans*, *trans*–*cis*, *trans* isomerization of HNNOH but the corresponding transition state lies 7·4 kcal mol^{-1} below the reactants. The $NH_2 + NO \rightarrow N_2H + OH$ channel is found to be endothermic by 1–3 kcal mol^{-1}. The calculated energy for the highest barrier for the $H_2 + N_2O$ product channel is 19·9 kcal mol^{-1} relative to $NH_2 + NO$, but Duan and Page [47] speculated that the best prediction of the net barrier to $H_2 + N_2O$ might be 9·2 kcal mol^{-1}. However, to reach the transition state for molecular H elimination requires a *cis* arrangement of the HNNO framework and, once it is attained, the barrier to water elimination is almost 30 kcal mol^{-1} lower than the barrier to molecular hydrogen elimination. Thus the third reaction channel is very unlikely to occur. Recent experimental results of Park and Lin [48] showed for the first time that the $NH_2 + NO$ reaction produced only $N_2H + OH$ and $N_2 + H_2O$ in the temperature range 302–1016 K with no evidence of a third product channel. This and other recent product branching measurements will be discussed later.

Diau *et al.* [49] carried out multichannel RRKM calculations using the *ab-initio* results of Walch [46]. The computed total rate constants exhibit a strong negative temperature dependence resulting primarily from the redissociation of the $H_2NNO^{\dagger}$ intermediate at higher temperatures because of the tight transition state for H migration to form HNNOH. The branching ratios for the two product channels $N_2H + OH$ (equation (3*a*)) and $N_2 + H_2O$ (equation (3*b*)) appear to be sensitive to the heat of the (3*a*) reaction channel. At 1000 K, the value varied from 0·17 to 0·68 when the heat of this channel changes from -1 to $+1$ kcal mol^{-1}.

Recently, Diau and co-workers [50–53] carried out a series of *ab-initio* and multichannel variational RRKM calculations for the $NH_2 + NO$ reaction. They studied nine isomers of the H_2N_2O species, 23 possible transition states and minimum-energy pathways for the barrierless bond-rupture processes at the B3LYP and CCSD(T) levels with various basis sets and at the G2M level. In general, their results on the reaction mechanism agree with those of Walch [46] as well as Duan and Page [47]. The CCSD(T)/6-311G(d, p) results of Diau and co-workers are a close match with Walch's CASSCF/ICCI results. Walch's data, adjusted by shifting $-5·9$ kcal mol^{-1} for all species with respect to the reactants based on the experimental enthalpy of the $NH_2 + NO \rightarrow N_2O + H_2$ reaction, are in agreement with the G2M predictions with uncertainties within ± 3 kcal mol^{-1}. The BAC-MP4 results of Melius and Binkley [33] are basically in agreement with the G2M data for the intermediates and products, but the relative energies predicted by BAC-MP4 for the transition states appear to be inaccurate due to the insufficient geometry optimization at the HF level of theory. Diau and Smith [51] found that the transition state for the five-centre H_2

elimination from *cis*, *cis*-HNNOH to form $H_2 + N_2O$ lies only 2·6 kcal mol^{-1} above the reactants, much lower than 9·2 kcal mol^{-1} estimated by Duan and Page [47]. On the other hand, this transition state is still 27·5 kcal mol^{-1} higher in energy than the transition state connecting HNNOH with the $H_2O + N_2$ products. Diau and Smith also investigated a reaction route leading to the *cis* and *trans*-NN(OH)H isomers which can be obtained from *trans*, *trans*-HNNOH via a loose transition state for the OH shift from one N to another. The barrier is about 50 kcal mol^{-1} and the transition state lies 2·3 kcal mol^{-1} higher than $NH_2 + NO$. NN(OH)H dissociates exothermically to $N_2 + H_2O$ without a substantial barrier and can produce $N_2H + OH$ endothermically without a reverse barrier. These workers suggested that the channel via NN(OH)H could be important for forming H_2O under high-temperature combustion conditions. The minimum-energy pathway study [52] showed that the HNNOH → NN(OH)H isomerization might occur via yet another, even looser transition state with the energy close to that of $N_2H + OH$. The endothermicity of the $N_2H + OH$ product channel calculated at the theory level as high as CCSD(T)/aug-PVQZ is 2·4 kcal mol^{-1}.

Using the microcanonical variational transition state theory (μVTST) in conjunction with the RRKM method, Diau and Smith [50] studied the temperature dependence of the rate coefficient and product branching ratios in the $NH_2 + NO$ reaction. The computed total rate coefficient displays a negative temperature dependence, in good agreement with direct kinetic measurements. The predicted values of the branching ratio for the formation of OH are strongly temperature dependent, increasing from 0·1 at room temperature to 0·85 at 3000 K. Sensitivity modelling indicates that the enthalpy of the $N_2H + OH$ products is a critical quantity for the branching ratio, as concluded earlier by Diau *et al.* [49]. The result, predicted by the μVTST at high temperatures, is consistent with the OH branching ratio obtained by NH_3–NO flame speed measurements by Vandooren *et al.* [54]. On the other hand, the theory substantially overestimates all available experimental data for the OH branching ratio in the 500–1200 K temperature range [50]. The reason for this deviation is still not clear. Diau *et al.* [53] also studied the pressure dependence and kinetic isotope effect for the rate constants and product branching ratios of each reaction channel. The pressure dependence of the total rate constant is estimated to be insignificant for the $NH_2 + NO$ reaction at $P < 200$ Torr and $T > 300$ K. However, a pressure effect is predicted for the $ND_2 + NO$ reaction under the same experimental conditions. The kinetic isotope effects of the total rate constant and the OH branching ratio are predicted to be small (5%) for the former and strong (a factor of two) for the latter.

Experimentally, the total rate constant and, in particular, the product branching ratios for the $NH_2 + NO$ reaction have been investigated in detail in our laboratory by pyrolysis–Fourier transform infrared spectrometry [55] as well as by pulsed-laser photolysis–mass spectrometry [48, 56]. These new results indicated that there are only two major product channels (3*a*) and (3*b*) up to 1200 K and the branching ratio for equation (3*a*) increases from 0·10 at 300 K to 0·28 at 1000 K, with a sharp upturn to $0{\cdot}45 \pm 0{\cdot}05$ at 1200 K, bridging nicely with the result of the NH_3–NO flame speed modelling by Vandooren *et al.* [54], about 0·5–0·9 from 1500 to 2000 K. This sigmoidal-type branching ratio for OH production cannot be satisfactorily accounted for by the μVRRKM calculations of Diau and Smith as mentioned above. One possibility is the opening of a new but related product channel HNNOH → NN(H)OH → H + N_2 + OH, analogous to $NN(OH)_2$ → OH + N_2 + OH, whose transition state has been identified in our $NH_2 + NO_2$ calculation, as discussed below.

4.2. $NH_2 + NO_2$

The reaction of NH_2 with NO_2 may also have various product channels:

$$NH_2 + NO_2 \rightarrow N_2O + H_2O, \quad \Delta H = -91{\cdot}5 \text{ kcal mol}^{-1}, \quad (4a)$$

$$\rightarrow H_2NO + NO, \quad \Delta H = -13{\cdot}3 \text{ kcal mol}^{-1}, \quad (4b)$$

$$\rightarrow N_2 + H_2O_2, \quad \Delta H = -85{\cdot}8 \text{ kcal mol}^{-1} \quad (4c)$$

$$\rightarrow N_2 + 2OH, \quad \Delta H = -36{\cdot}2 \text{ kcal mol}^{-1}, \quad (4d)$$

$$\rightarrow 2HNO, \quad \Delta H = -5{\cdot}8 \text{ kcal mol}^{-1}. \quad (4e)$$

Earlier, only the channel (4*b*) was studied theoretically by Saxon and Yoshimine [57] at the MRCI/6-31G*//CASSCF/4-31G level as well as by Seminario and Politzer [58] who used a density functional approach. Melius [59] has calculated the heats of formation for some intermediates and transition states using his BAC-MP4 method. Recently, we reported a comprehensive study on a variety of mechanisms at the G2 level of theory [60]. The PES of $NH_2 + NO_2$ for the two major product channels (4*a*) and (4*b*) is shown in figure 2(*b*).

The channels producing $H_2NO + NO$ are shown to be the following:

(i) $NH_2 + NO_2 \rightarrow H_2NNO_2 \rightarrow H_2NONO \rightarrow H_2NO + NO$, taking place by the association of the reactants to form the NN bond, the nitro-nitrite rearrangement and the ON bond scission;

(ii) $NH_2 + NO_2 \rightarrow H_2NONO \rightarrow H_2NO + NO$, occurring by the association of H_2N with ONO forming the NO bond and the ON bond scission.

In mechanism (i), the barrier for nitro-nitrite rearrangement, 31·2 kcal mol^{-1} with respect to H_2NNO_2, is 20·8 kcal mol^{-1} lower than the energy for the NN bond scission back to $NH_2 + NO_2$. The first association steps are calculated to be highly exothermic, by 52·0 and 34·1 kcal mol^{-1} for H_2NNO_2 and H_2NONO respectively and do not have barrier for either intermediate. Channel (ii) is analogous to the $NH + NO_2 \rightarrow HNONO \rightarrow HNO + NO$ channel of the $NH + NO_2$ reaction.

Thermodynamically, the most stable $N_2O + H_2O$ products can be formed in this reaction by a complex mechanism (iii) namely $NH_2 + NO_2 \rightarrow H_2NNO_2 \rightarrow$ *trans*, *cis*-HNN(OH)O (*trans*-HNNO(H) and *cis*-NNOH) $\rightarrow$ *trans*, *trans*-HNN(OH)O $\rightarrow$ *cis*, *trans*-HNN(OH)O $\rightarrow N_2O + H_2O$, involving first formation of H_2NNO_2, the 1,3-H shift from N to O, rotation of the OH bond, H shift from one O to another and migration of the second H atom from N to O, leading to elimination of H_2O. The rate-determining step for this mechanism starting from H_2NNO_2 is 1,3-H shift, and the corresponding transition state lies 12·5 kcal mol^{-1} below the reactants but 8·3 kcal mol^{-1} higher than the transition state for the nitro-nitrite rearrangement. The highest energy transition states in mechanism (iii) involve migration of a H atom. Therefore, tunnelling corrections are expected to be important for rate-constant calculations. The mechanism for the formation of $N_2O + H_2O$ is similar to that of $N_2 + H_2O$ in the $NH_2 + NO$ reaction, except for other details as discussed below.

Aside from the two major product channels mentioned above, the $N_2 + 2OH$ products can be formed by several reaction mechanisms; however, all of them involve $NN(OH)_2$, formed by the second 1,3-H shift from N to O which have high barriers. The transition state for this second 1,3-H shift lies 6·9 kcal mol^{-1} above the reactants and much higher than the rate-controlling transition states for the channels producing $H_2NO + NO$ and $N_2O + H_2O$. The decomposition of $NN(OH)_2$ producing $N_2 + 2OH$ may take place directly via a loose transition state with C_1 symmetry or by a stepwise

mechanism $NN(OH)_2 \rightarrow NNOH + OH \rightarrow N_2 + 2OH$. There is no channel producing $N_2 + HOOH$ directly from the reactants; HOOH can be produced only by recombination of 2OH.

Complex variational RRKM calculations would be necessary to obtain the rate constants of channels (i), (ii) and (iii), and to predict the product branching ratio. The potential energy profile suggests that the channels producing $H_2NO + NO$ should compete favourably with the channels producing $N_2O + H_2O$. Recent experimental measurements by us [61, 62] and by Quandt and Hershberger [63] confirmed our theoretical conclusion. The result of kinetic modelling by Glarborg *et al.* [64] for the reaction of ammonia with nitrogen dioxide in a flow reactor in the 850–1350 K temperature range also supports the conclusion. In a most comprehensive study to date by laser photolysis–mass spectrometry by Park and Lin [61, 62] for the temperature range 300–1000 K, they concluded that the branching ratio for the formation of $N_2O + H_2O$ is $0{\cdot}19 \pm 0{\cdot}02$, independent of temperature. This result contradicts that of Meunier *et al.* [65], 0·59 at room temperature, which may have been seriously compromised by the presence of secondary NH and N reactions.

The $NH_x + NO_x$ ($x = 1, 2$) reactions have much in common. All of them are fast at room temperature with the rate constants in the $(1{\cdot}0–6{\cdot}0) \times 10^{-11}$ cm^3 molecule^{-1} s^{-1} range and exhibit a negative temperature dependence. All the reactions have an initial exothermic association step occurring without barrier. Then, they proceed by H shifts and internal rearrangements in $H_xNNO_x^{\ddagger}$ followed by the elimination of H, OH or H_2O. The barriers for isomerization and dissociation of H_xNNO_x can be high but, for the most important channels, their transition states lie below the reactants, which explains the negative temperature dependence of the rate coefficients. Among the H_xNNO_x species, the NN bond is strongest in HNNO (56 kcal mol^{-1}), followed H_2NNO_2 (52 kcal mol^{-1}) and H_2NNO (47 kcal mol^{-1}), and is weakest in $HNNO_2$ (38 kcal mol^{-1}). For the NO_2 reactions, the initial association can lead to formation of NO bonds. The NO bonds have similar strengths of 34–35 kcal mol^{-1} in both HNONO and H_2NONO. In this case, the reactions produce the NO radical. Overall, among the products of $NH_x + NO_x$ ($x = 1, 2$), there are stable molecules N_2, N_2O, H_2O and HNO, as well as free radicals H, OH, NO and H_2NO. The product branching ratio is specific for each particular reaction and controlled by the potential energy surface.

5. $NH_3 + NO_x$ reactions

The reactions of NH_3 with NO and NO_2 differ from those of NH and NH_2. The $NH_3 + NO_x$ reactions are endothermic and proceed by abstraction of H atom from NH_3 by the NO_x radicals to form HNO_x and NH_2. In particular,

$$NH_3 + NO \rightarrow NH_2 + HNO \tag{5}$$

has a high endothermicity, about 58 kcal mol^{-1}. These reactions are important because their reverse processes, $NH_2 + HNO_x$ ($x = 1, 2$), are ubiquitous in the H, N, O system and there have been no kinetic data available for modelling applications.

Recently [66], we investigated the PES for the $NH_3 + NO$ reaction using the G2 approach with UMP2/6-311 G** optimized geometries. We found a loose transition state for H abstraction with the geometry close to that of the products. The N(O)–H and N(H_2)–H distances are 1·12 and 1·53 Å respectively, and the NHN angle is 167·9°. At the UMP2/6-311G** level with ZPE correction the barrier is 61·4 kcal mol^{-1}, about 1 kcal mol^{-1} for the reverse reaction. However, at the G2 level, the energy of the transition state is lower than that of the $NH_2 + HNO$ products, that is the reverse

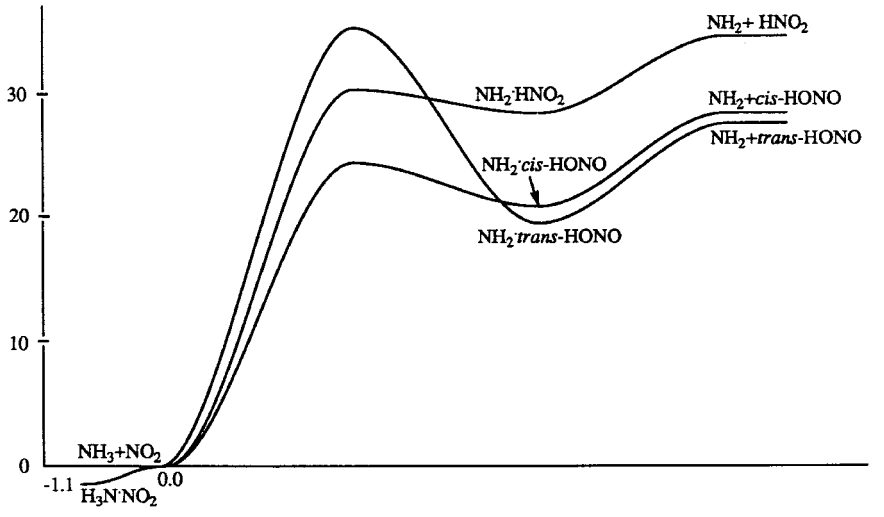

Figure 3. Calculated profile of the PES for the reaction $NH_3 + NO_2$.

barrier disappears. We studied the reaction path between the reactants and products using the intrinsic reaction coordinate calculations. The calculated PES and molecular parameters for the structures along the reaction path were used for variational transition state theory (VTST) calculations of the rate constants. The following three-parameter expression was obtained for k_5 for the temperature range 300–5000 K:

$$k_5 = 1{\cdot}72 \times 10^{-17}\, T^{1{\cdot}73} \exp\left(\frac{-28\,454}{T}\right) \text{cm}^3\ \text{molecule}^{-1}\ \text{s}^{-1}.$$

The value of k_5 estimated by Hanson and co-workers [67] from their shock tube study, $8{\cdot}3 \times 10^{-10}$ exp $(-25\,161/T)$ cm^3 molecule^{-1} s^{-1} is significantly higher than our calculated value. However, the rate constant obtained by Hanson and co-workers does not seem to be reliable because they used an estimate for activation energy of 50·0 kcal mol^{-1}, much lower than the experimental reaction endothermicity. In our k_5, the apparent activation energy, 58·3 kcal mol^{-1}, calculated variationally for the temperature range 300 K $\leqslant$ 1000 K, is close to the experimental enthalpy change 58·5 kcal mol^{-1}. The calculated equilibrium constant for reaction (5), $K_5 = 6{\cdot}34 \exp(-29\,084/T)$, is close to that computed on the basis of JANAF tables, $K_5 = 9{\cdot}21 \exp(-29\,603/T)$.

We have also studied [66] the reaction

$$NH_3 + NO_2 \rightarrow NH_2 + HONO \qquad (6)$$

which is endothermic by 29–30 kcal mol^{-1} for *trans*- and *cis*-HONO. The energies of the reactants, intermediate complexes, transition states and products were computed with the Gaussian-1 (G1) scheme [6] using the UMP2/6-311G** and B3LYP/6-311G** levels of theory for structural optimization and frequency calculations. The PES is shown in figure 3. Reaction (6) can occur by three channels, leading to HNO_2 (6*a*), *cis*-HONO (6*b*) and *trans*-HONO (6*c*). All three mechanisms involve two steps: firstly abstraction of H from NH_3 with the formation of $NH_2 \cdot HNO_2$ or $NH_2 \cdot HONO$ complexes; secondly dissociation of the complexes. The first step has the barriers of 31·8, 24·6 and 35·5 kcal mol^{-1} at the G1 level for channels (6*a*), (6*b*) and (6*c*),

respectively. Thus mechanism (6*a*) producing *cis*-HONO is expected to be dominant for the reaction. The complexes of NH_2 with various isomers of HNO_2 species are stabilized by 6–7 kcal mol^{-1} with respect to the products and dissociate without barrier. For channels (6*a*) and (6*b*) the abstraction transition states lie below the products in energy, and the second step is rate controlling at low temperatures. However, at ambient temperature and higher, the entropy contribution makes the first H abstraction step rate determining; the Gibbs free energies of the abstraction transition states are higher than that of products. Therefore the VTST rate constants for reactions (6*a*) and (6*b*) were calculated using molecular parameters of the transition states for the first reaction step. VTST calculations of the rate constants for the dominant channel (6*b*) were carried out with G1 energies and UMP2 or B3LYP molecular parameters. UMP2 gave rise to a significantly tighter transition state structure than B3LYP, resulting in a much smaller rate constant:

$$k_{6b}(\mathrm{UMP2}) = 1{\cdot}22 \times 10^{-23}\, T^{3{\cdot}30} \exp\left(\frac{-11\,217}{T}\right) \mathrm{cm^3\ molecule^{-1}\ s^{-1}},$$

$$k_{6b}(\mathrm{B3LYP}) = 1{\cdot}96 \times 10^{-23}\, T^{3{\cdot}41} \exp\left(\frac{-11\,301}{T}\right) \mathrm{cm^3\ molecule^{-1}\ s^{-1}},$$

for the temperature range 300–3000 K. A similar calculation made with the B3LYP structure, frequencies and G2M energies by Thaxton *et al.* [68], resulted in the rate constant which lay between the above two values. The G2M result agreed closely with kinetically modelled rate constant for the $NH_3 + NO_2 \rightarrow NH_2 + HONO$ reaction, $k_6 = 4{\cdot}1 \times 10^{-13} \exp(-12\,620/T)$ cm^3 molecule^{-1} s^{-1}. The theoretical activation energy, E_a = 25·6 kcal mol^{-1}, evaluated with data below 1000 K, where most reliable experiments for the abstraction process have been carried out, agrees almost exactly with the experimental value as given, 25·2 kcal mol^{-1}. The calculated equilibrium constants

$$K_{6b}(\mathrm{UMP2}) = 7{\cdot}29 \exp\left(\frac{-14\,131}{T}\right),$$

$$K_{6b}(\mathrm{B3LYP}) = 7{\cdot}54 \exp\left(\frac{-14\,133}{T}\right),$$

agree fairly well with the JANAF equilibrium constant [66]

$$K_{6b} = 8{\cdot}87 \exp\left(\frac{-15\,524}{T}\right).$$

For the slower channels (6*a*) and (6*c*), the calculations give the following rate constants:

$$k_{6a} = 4{\cdot}07 \times 10^{-24}\, T^{3{\cdot}41} \exp\left(\frac{-15\,036}{T}\right) \mathrm{cm^3\ molecule^{-1}\ s^{-1}},$$

$$k_{6c} = 3{\cdot}12 \times 10^{-23}\, T^{3{\cdot}52} \exp\left(\frac{-16\,404}{T}\right) \mathrm{cm^3\ molecule^{-1}\ s^{-1}}.$$

6. Concluding remarks

In this review, we have summarized the results of recent theoretical studies on the reactions of NO_x (x = 1, 2) with nitrogen hydrides (NH_y, y = 1–3) using various levels of theory. For the radical–radical processes, $NH_x + NO_x$ (x = 1, 2), despite the

absence of quantitative treatment for the association steps in the majority of studies presented, detailed information on the subsequent isomerization and decomposition of excited association products are now available. Most recent results, based on multireference configuration interaction, CASSCF and various types of G2 calculation agree reasonably well within 3–5 kcal mol^{-1} for the intermediates and the transition states connecting those intermediates.

The key challenge remains in our ability to predict quantitatively the absolute rate constants for the initial association reactions as well as for the formation of various products as functions of temperature and pressure. For example, the $NH_x + NO_x$ reactions are relevant to the de-NO_x process and the combustion of propellants such as ADN. Can we reliably predict their absolute rate constants and product branching ratios under 1 atm at 1200–1400 K and/or 200 atm at 1500–2000 K? These questions, which are raised frequently by the combustion community, require considerably more effort by experimentalists and theoreticians in several respects. Firstly we need more accurate product branching ratio measurements for improvement in PESs, particularly for the initial association and final fragmentation processes. Secondly the deactivation of the chemically activated associated products play important roles in the overall kinetics. We nee a reliable model for the quantitative description of the collisional quenching step so as to predict quantitatively the deactivation as against the isomerization–decomposition rates. For the NH_x–NO_x systems, the latter processes involve the motion of the H atom in the transition states. Accordingly, our ability to describe the population of the partially deactivated association intermediates so as to calculate their tunnelling rates is critical.

For the metathetical reactions of NO_x with NH_3, we have reviewed the results calculated by different Gaussian methods (G1, G2 and G2M). For the $NH_3 + NO_2 \rightarrow NH_2 + HONO$ reaction, for which we recently obtained an absolute rate constant, the computed TST value based on the G2M energies of the reactants and the transition state agrees quantitatively with the kinetically modelled result.

Acknowledgements

The authors gratefully acknowledge the support of this work by the Office of Naval Research (contract No. N00014-89-J-1949) under the direction of Dr R. S. Miller.

References

[1] Lyon, R. K., 1976, *Int. J. chem. Kinet.*, **8**, 318; 1975, US patent 3900554.
[2] Parry, R. A., and Siebers, D. L., 1986, *Nature*, **324**, 657.
[3] Brill, T. B., Brush, P. J., and Patil, D. G., 1993, *Combust. Flame*, **92**, 7788; Mebel, A. M., Lin, M. C., Morokuma, K., and Melius, C. F., 1995, *J. phys. Chem.*, **99**, 6842.
[4] Borman, S., 1994, *Chem. Engng News*, **72**, 18.
[5] Baulch, D. L., Cobos, C. J., Cox, R. A., Esser, C., Frank, P., Just, Th., Kerr, J. A., Pilling, M. J., Troe, J., Walker, R. W., and Warnatz, J. J., 1992, *J. phys. chem. Ref. Data*, **21**, 411.
[6] Curtiss, L. A., Raghavachari, K., Trucks, G. W., and Pople, J. A., 1991, *J. chem. Phys.*, **94**, 7221; Pople, J. A., Head-Gordon, M., Fox, D. J., Raghavachari, K., and Curtiss, L. A., 1989, *J. chem. Phys.*, **90**, 5622; Curtiss, L. A., Jones, C., Trucks, G. W., Raghavachari, K., and Pople, J. A., 1990, *J. chem. Phys.*, **93**, 2537; Curtiss, L. A., Raghavachari, K., Trucks, G. W., and Pople, J. A., 1993, *J. chem. Phys.*, **98**, 1293; Curtiss, L. A., Redfern, P. C., Smith, B. J., and Radom, L., 1996, *J. chem. Phys.*, **104**, 5148.
[7] Mebel, A. M., Morokuma, K., and Lin, M. C., 1995, *J. chem. Phys.*, **103**, 7414.
[8] Pople, J. A., Head-Gordon, M., and Raghavachari, K., 1987, *J. chem. Phys.*, **87**, 5698.

[9] Hehre, W., Radom, L., Schleyer, P. v. R., and Pople, J. A., 1986, *Ab Initio Molecular Orbital Theory* New York: Wiley).
[10] Durant, J. L., and Rohlfing, C. M., 1993, *J. chem. Phys.*, **98**, 8031.
[11] Becke, A. D., 1992, *J. Chem. Phys.*, **97**, 9173; 1992, *Ibid.*, **98**, 21155; 1993, *Ibid.*, **98**, 5648.
[12] Lee, C., Yang, W., and Parr, R. G., 1988, *Phys. Rev.* B, **37**, 785.
[13] Liu, R., Morokuma, K., Mebel, A. M., and Lin, M. C., 1996, *J. phys. Chem.*, **100**, 9314.
[14] Hsu, C.-C., Mebel, A. M., and Lin, M. C., 1996, *J. chem. Phys.*, **105**, 2346.
[15] Mebel, A. M., Lin, M. C., Morokuma, K., and Melius, C. F., 1996, *Int. J. chem. Kinet.*, **28**, 693.
[16] Mebel, A. M., Diau, E. W. G., Lin, M. C., and Morokuma, K., 1996, *J. Am. chem. Soc.*, **118**, 9759.
[17] Gordon, S., Mulac, W., and Nangian, P., 1971, *J. phys. Chem.*, **75**, 2087.
[18] Hansen, I., Höinghaus, K., Zetzsch, C., and Stuhl, F., 1976, *Chem. Phys. Lett.*, **47**, 370.
[19] Cox, J. W., Nelson, H. H., and McDonald, J. R., 1986, *Chem. Phys.*, **96**, 175.
[20] Harrison, J. A., Whyte, A. R., and Phillips, L. F., 1986, *Chem. Phys. Lett.*, **129**, 346.
[21] Yamasaki, K., Okada, S., Koshi, M., and Matsui, H., 1991, *J. chem. Phys.*, **95**, 5087.
[22] Okada, S., Miyoshi, A., and Matsui, H., 1994, *J. chem. Phys.*, **101**, 9582.
[23] Mertens, J. D., Chang, A. Y., Hanson, K., and Bowman, C. T., 1991, *Int. J. chem. Kinet.*, **23**, 173.
[24] Yokoyama, K., Sakane, Y., and Fueno, T., 1991, *Bull. chem. Soc. Japan*, **64**, 1738.
[25] Dean, A. M., Chou, M.-S., and Stern, D., 1984, *Int. J. chem. Kinet.*, **16**, 633.
[26] Vandooren, J., Sarkisov, O. M., Balakhnin, V. P., and van Tiggelen, P. J., 1991, *Chem. Phys. Lett.*, **184**, 294.
[27] Durant, J. L., Jr, 1994, *J. phys. Chem.*, **98**, 518.
[28] Wolf, M., Yang, D. L., and Durant, J. L., Jr., 1994, *J. Photochem. Photobiol.* A, **80**, 85.
[29] Durant, J. L., Jr., 1995, *Research in Chemical Kinetics*, edited by R. G. Compton and G. Hancock (Amsterdam: Elsevier), p. 69.
[30] Quandt, R. W., and Hershberger, J. F., 1995, *J. phys. Chem.*, **99**, 16939.
[31] Patel-Mistra, D., and Dagdigian, P. J., 1992, *J. phys. Chem.*, **96**, 3232.
[32] Böhmer, E., Shin, S. K., Chen, Y., and Wittig, C., 1992, *J. chem. Phys.*, **97**, 2536.
[33] Melius, C. F., and Binkley, J. S., 1984, *Symp.* (*Int.*) *Combust.*, [*Proc.*], **20**, 575.
[34] Miller, J. A., and Melius, C. F., 1993, *Symp.* (*Int.*) *Combust.*, [*Proc.*], **24**, 719.
[35] Fueno, T., Fukuda, M., and Yokoyama, K., 1988, *Chem. Phys.*, **124**, 265.
[36] Harrison, J. A., and Maclagan, R. G. A. R., 1990, *J. chem. Soc., Faraday Trans.*, **86**, 3519.
[37] Walch, S. P., 1993, *J. chem. Phys.*, **98**, 1170.
[38] Bradley, K. S., McCabe, P., Schatz, G. C., and Walch, S. P., 1995, *J. chem. Phys.*, **102,** 6696.
[39] Mebel, A. M., Morokuma, K., and Lin, M. C., 1994, *J. chem. Phys.*, **101**, 3916.
[40] Mebel, A. M., Lin, M. C., Morokuma, K., and Melius, C. F., 1996, *Int. J. chem. Kinet.*, **28**, 693.
[41] Silver, J. A., and Kolb, C. E., 1982, *J. phys. Chem.*, **86**, 3240.
[42] Silver, J. A., and Kolb, C. E., 1987, *J. phys. Chem.*, **91**, 3713.
[43] Casewit, C. J., and Goddard, W. A., III, 1982, *J. Am. Chem. Soc.*, **104**, 3280.
[44] Abou-Rachid, H., Pouchan, C., and Chaillet, M., 1984, *Chem. Phys.*, **90**, 243.
[45] Harrison, J. A., Maclagan, R. G. A. R., and Whyte, A. R., 1987, *J. phys. Chem.*, **91**, 6683.
[46] Walch, S. P., 1993, *J. chem. Phys.*, **99**, 5295.
[47] Duan, X., and Page, M., 1995, *J. molec. Struct.* (*Theochem.*), **333**, 233.
[48] Park, J., and Lin, M. C., 1996, *J. phys. Chem.*, **100**, 3317.
[49] Diau, E. W., Yu, T., Wagner, M. A. G., and Lin, M. C., 1994, *J. phys. Chem.*, **98**, 4034.
[50] Diau, E. W.-G., and Smith, S. C., 1996, *J. phys. Chem.*, **100**, 12349.
[51] Diau, E. W.-G., and Smith, S. C., 1997, *J. chem. Phys.* (submitted).
[52] Diau, E. W.-G., Smith, S. C., Hu, C.-H., and Schaefer, H. F., III, 1997, *J. chem. Phys.* (submitted).
[53] Diau, E. W.-G., Smith, S. C., Yang, D. L., and Durant, J. L., 1997 (to be published).
[54] Vandooren, J., Bian, J., and van Tiggelen, P. J., 1994, *Combust. Flame*, **98**, 402.

[55] HALBGEWACHS, M. J., DIAU, E. W. G., MEBEL, A. M., LIN, M. C., and MELIUS, C. F., 1997, *Symp.* (*Int.*) *Combust.*, [Proc.], **26** (to be published).
[56] PARK, J., and LIN, M. C., 1997, *J. phys. Chem.* A, **101**, 5.
[57] SAXON, R. P., and YOSHIMINE, M., 1989, *J. phys. Chem.*, **93**, 3130.
[58] SEMINARIO, J., and POLITZER, P., 1992, *Int. J. quant. Chem. Symp.*, **26**, 497.
[59] MELIUS, C. F., 1986, *BAC Heats of Formation and Free Energies* (Livermore, California: Sandia National Laboratories).
[60] MEBEL, A. M., HSU, C.-C., LIN, M. C., and MOROKUMA, K., 1995, *J. chem. Phys.*, **103**, 5640.
[61] PARK, J., and LIN, M. C., 1996, *Int. J. chem. Kinet.*, **28**, 879.
[62] PARK, J., and LIN, M. C., 1997, *J. phys. Chem.* (submitted).
[63] QUANDT, R. W., and HERSHBERGER, J. F., 1996, *J. Phys. Chem.*, **100**, 9407.
[64] GLARBORG, P., DAM-JOHANSEN, K., and MILLER, J. A., 1995, *Int. J. chem. Kinet.*, **27**, 1207.
[65] MEUNIER, J., PAGSBERG, P., and SILLESEN, A., 1996, *Chem. Phys. Lett.*, **261**, 277.
[66] MEBEL, A. M., DIAU, E. W. G., LIN, M. C., and MOROKUMA, K., 1996, *J. phys. Chem.*, **100**, 7517.
[67] ROOSE, T. R., HANSON, R. K., and KRUGER, C. H., 1978, *Proceedings of the 11th International Symposium Shock Tube and Shock Wave Research*, **11**, 245.
[68] THAXTON, A. G., HSU, C.-C., and LIN, M. C., 1997, *Int. J. chem. Kinet.* (to be published).